



Constrained least-squares optimization for robust estimation of center of rotation

Lillian Y. Chang*, Nancy S. Pollard

School of Computer Science, Carnegie Mellon University, Pittsburgh, Pennsylvania, USA

Accepted 7 May 2006

Abstract

This paper presents a new direct method for estimating the average center of rotation (CoR). An existing least-squares (LS) solution has been shown by previous works to have reduced accuracy for data with small range of motion (RoM). Alternative methods proposed to improve the CoR estimation use iterative algorithms. However, in this paper we show that with a carefully chosen normalization scheme, constrained least-squares solutions can perform as well as iterative approaches, even for challenging problems with significant noise and small RoM. In particular, enforcing the normalization constraint avoids poor fits near plane singularities that can affect the existing LS method. Our formulation has an exact solution, accounts for multiple markers simultaneously, and does not depend on manually-adjusted parameters. Simulation tests compare the method to four published CoR estimation techniques. The results show that the new approach has the accuracy of the iterative methods as well as the short computation time and repeatability of a least-squares solution. In addition, application of the new method to experimental motion capture data of the thumb carpometacarpal (CMC) joint yielded a more plausible CoR location compared to the previously reported LS solution and required less time than all four alternative techniques.

© 2006 Elsevier Ltd. All rights reserved.

Keywords: Center of rotation; Joint center; Least-squares; Optimization

1. Introduction

Modeling human joint kinematics from non-invasive surface measurements is a key component of biomechanical motion analysis. Anatomical joints of the human body are often approximated by idealized spherical and axial joints. The center of rotation (CoR) of these joint models are required for measuring skeletal parameters and determining joint angles to describe a particular subject's motion.

This paper focuses on functional methods, which infer the CoR from the relative motion of adjacent body

segments (e.g. Silaghi et al., 1998; Halvorsen et al., 1999; Piazza et al., 2001; Gamage and Lasenby, 2002; Marin et al., 2003; Halvorsen, 2003; Zhang et al., 2003; Cerveri et al., 2005), rather than predictive methods, which calculate the CoR from empirical relations between specific anatomical landmarks (e.g. Bell et al., 1989; Kadaba et al., 1990; Davis et al., 1991; Vaughan et al., 1999). Several functional methods use cost function minimization to fit the joint model to measured marker trajectories. The selected cost function determines whether the optimal solution can be calculated exactly or only approximated by successive iterative steps toward the optimum CoR value.

Halvorsen et al. (1999), Gamage and Lasenby (2002), and Pratt (1987) use least-squares (LS) methods which give exact CoR estimation techniques. Halvorsen et al. (1999) adapts the Reuleaux construction for computing

*Corresponding author. The Robotics Institute, Carnegie Mellon University, 5000 Forbes Avenue, Pittsburgh, PA 15213, USA.
Tel.: +1 412 268 7895.

E-mail address: lillianc@ri.cmu.edu (L.Y. Chang).

a single instantaneous CoR (Reuleaux, 1876; Panjabi, 1979) to estimate the average CoR simultaneously from multiple displacements, but the algorithm requires a choice of frame separation. Gamage and Lasenby (2002) derive a LS method to fit marker trajectories to a sphere which requires no parameter adjustments and was shown to have improved consistency and accuracy compared to the Halvorsen et al. (1999) method. The Cholesky decomposition simple fit developed by Pratt (1987) is equivalent to this solution for the case of a single marker. However, the Gamage and Lasenby (2002) solution and the Cholesky decomposition method is considerably less accurate in cases of reduced joint range of motion (RoM), as shown in previous studies both analytically (Pratt, 1987; Halvorsen, 2003) and empirically (Pratt, 1987; Halvorsen, 2003; Marin et al., 2003; Cerveri et al., 2005).

Alternative approaches for CoR estimation have primarily been iterative. Halvorsen (2003) derives a bias compensation (BC) algorithm to re-estimate the CoR from the LS sphere fit of Gamage and Lasenby (2002). The methods of Silaghi et al. (1998), Piazza et al. (2001), and Cerveri et al. (2005) also use sphere fitting but differ in the cost function, use of weighting factors, and choice of iterative search (IS) algorithm. The minimal amplitude (MA) point method (Marin et al., 2003) does not fit data to a sphere but instead models the CoR as the point with the least movement in the fixed frame. Zhang et al. (2003) estimate finger segmental CoRs by optimizing a cost function derived from a parameterized relationship between joint angle and surface marker excursion. The major disadvantage of these iterative approaches is the potential for different solutions depending on the existence of local minima in the cost function and values of optimization parameters such as convergence criterion, weights, and initialization. In addition, the methods developed by Marin et al. (2003) and Zhang et al. (2003) are limited by their computational expense.

This work presents a new sphere-fitting method whose solution is both exact and accurate even for reduced RoM. An analysis of two candidate cost functions first shows why the LS solution of Gamage and Lasenby (2002) may lead to inaccurate CoR estimates. We then present the sphere-fitting technique developed by Pratt (1987) to introduce the framework for our constrained LS approach and note the critical role of an appropriate normalization constraint (Pratt, 1987). This technique only applies to the case of a single marker, however. We then extend the method for fitting multiple marker trajectories which share a common CoR but have different radii. The insight developed from the single marker analysis leads to a normalization constraint for multiple markers which maintains good fits even for small ranges of motion (RoMs).

2. Cost function analysis

We assume that markers attached to a body segment maintain a constant distance from a fixed CoR but do not necessarily exhibit rigid body motion relative to each other. Therefore, we use a non-rigid sphere-fitting approach; the spherical fit should have minimal variation in the separation length between the CoR \mathbf{m} and the p th marker position at the k th frame, \mathbf{v}_k^p (Fig. 1).

One formulation of error from the spherical surface is the geometric, or Euclidean, distance ε_k^p defined by the difference between the marker distance from the center and the nominal radius for the p th marker, r_p :

$$\varepsilon_k^p = \sqrt{\|\mathbf{v}_k^p - \mathbf{m}\|^2} - r_p. \quad (1)$$

A least-squares cost function f_1 for minimizing the overall geometric error becomes

$$f_1 = \sum_{p=1}^P \sum_{k=1}^N (\varepsilon_k^p)^2 = \sum_{p=1}^P \sum_{k=1}^N \left(\sqrt{\|\mathbf{v}_k^p - \mathbf{m}\|^2} - r_p \right)^2 \quad (2)$$

for the entire data set of P markers and N frames. The closed-form expression of r_p at the optimal solution is found by setting the derivative of Eq. (2) with respect to r_p equal to zero. However, there is no closed-form solution for the CoR since \mathbf{m} is within the radicand of Eq. (2). An IS routine is hence required to minimize this particular cost function, similar to the approaches of Silaghi et al. (1998), Piazza et al. (2001), and Cerveri et al. (2005).

Gamage and Lasenby (2002) instead model the radial variation by the difference of the squared lengths

$$\delta_k^p = \|\mathbf{v}_k^p - \mathbf{m}\|^2 - (r_p)^2 \quad (3)$$

used in the corresponding least-squares cost function f_2 :

$$f_2 = \sum_{p=1}^P \sum_{k=1}^N (\delta_k^p)^2 = \sum_{p=1}^P \sum_{k=1}^N (\|\mathbf{v}_k^p - \mathbf{m}\|^2 - (r_p)^2)^2. \quad (4)$$

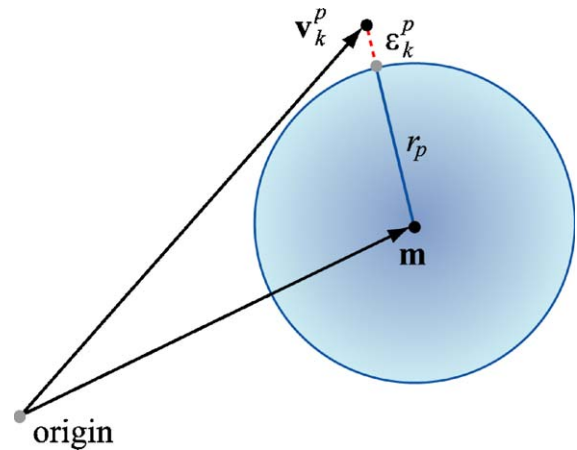


Fig. 1. Model of the p th marker at time k around a spherical joint. The marker position \mathbf{v}_k^p is on the surface of a sphere with center \mathbf{m} and nominal radius r_p , with some geometric error ε_k^p .

The quadratic form of Eq. (4) allows an exact solution for \mathbf{m} (Gamage and Lasenby, 2002). We can write the relationship between the two cost metrics by using Eqs. (1) and (3) to re-write δ_k^p in terms of ε_k^p and r_p for a given set of marker positions, average CoR, and marker radii:

$$(\delta_k^p)^2 = ((\varepsilon_k^p)^2 + 2\varepsilon_k^p r_p)^2. \quad (5)$$

Eq. (5) shows that the error metric used by Gamage and Lasenby (2002) is a function of both the geometric error ε_k^p and the estimated trajectory radius r_p . Thus, minimizing the cost function in Eq. (4) will favor solutions which have not only small geometric error but also smaller radius estimates in some circumstances. In practice, this results in underestimation of the radius r_p when the data has reduced RoM. Also see the work by Pratt (1987) and Halvorsen (2003), who explain the corresponding CoR inaccuracy using different mathematical perspectives.

Our proposed method minimizes a cost function similar to that in Eq. (4) such that we have an exact solution. However, we show that by using a properly-normalized cost function, we can achieve much better results for data sets having small RoM.

3. Method for a single marker

Non-rigid sphere fitting of a single marker trajectory is a specific application of the method developed by Pratt (1987) for direct fitting of general algebraic surfaces. A point $\mathbf{v} = (x, y, z)^T$ on the surface of a sphere with center $\mathbf{m} = (x_c, y_c, z_c)^T$ and radius r satisfies the following equation exactly:

$$(x - x_c)^2 + (y - y_c)^2 + (z - z_c)^2 - (r)^2 = 0. \quad (6)$$

Eq. (6) can be rewritten to use basis function coefficients $\mathbf{u} = (a, b, c, d, e)^T$ rather than \mathbf{m} and r to define the sphere:

$$aw + bx + cy + dz + e = 0, \quad (7)$$

where w is the basis function $x^2 + y^2 + z^2$. The five coefficients in \mathbf{u} correspond to the five basis functions $(w, x, y, z, 1)$. The algebraic distance δ evaluates how well the fit \mathbf{u} describes a data point \mathbf{v} :

$$\delta(\mathbf{u}) = (w, x, y, z, 1)^T \mathbf{u}. \quad (8)$$

Note that the algebraic distance is equivalent to the error function in Eq. (3) scaled by the parameter a . We will estimate the sphere fit which minimizes the sum of squared algebraic distances over every time frame, which is equivalent to Eq. (4) scaled by the parameter a^2 for a single marker.

3.1. Normalization constraint selection

The relative, rather than absolute, values of the polynomial coefficients in \mathbf{u} determine the estimated sphere center and radius, so that a is a free parameter which can be set to constrain the cost function. In fact, any function of the coefficients in \mathbf{u} can be specified as a normalization function to constrain the arbitrary scaling of the algebraic distance. The choice of constraint is critical to the quality of the fit because every normalization scheme has singularities which are impossible to fit, and solutions near these singularities are poorly behaved (Pratt, 1987).

For example, the Cholesky decomposition simple fit (Pratt, 1987) uses the constraint $a = 1$. With this normalization function, the algebraic distance defined in Eq. (8) reduces to the same error metric used by the LS solution in Gamage and Lasenby (2002), and the CoR estimates would be identical. However, data sets whose solution \mathbf{u} has $a = 0$ are unfittable under the $a = 1$ normalization constraint. Note that the singularity $a = 0$ reduces Eq. (7) to the equation of a plane. The effect in practice is that marker trajectories with a small RoM and large error are near the plane singularities and will be poorly fit, as confirmed empirically by Pratt (1987), Marin et al. (2003), Halvorsen (2003), and Cerveri et al. (2005). Pratt (1987) develops an alternative normalization constraint to avoid singularities near good-fit candidates for \mathbf{u} :

$$b^2 + c^2 + d^2 - 4ae = 1. \quad (9)$$

For some intuition, we compare Eqs. (6) and (7) to re-write Eq. (9) as

$$a^2 r^2 = 1. \quad (10)$$

The normalization constraint is a function of the scaling parameter and the radius only. Because it does not depend on the CoR location represented by parameters b, c , and d , it is invariant under translation and rotation of the data set coordinate system. Furthermore, using Eq. (10) with Eq. (8), we can write the expression for squared algebraic distance as

$$\delta^2 = a^2 (\varepsilon^2 + 2\varepsilon r)^2 = \frac{1}{r^2} (\varepsilon^2 + 2\varepsilon r)^2 = \left(\frac{\varepsilon^2}{r} + 2\varepsilon \right)^2. \quad (11)$$

The dependence on radius r is relocated to the quadratic ε^2 term compared to Eq. (5), which reduces the potential for radius underestimation compared to the $a = 1$ constraint.

For this normalization scheme, the only singularities occur for zero-radius spheres at a single point. Such a situation corresponds to a marker placed nearly coincident with the CoR, a condition which does not occur in practical motion capture applications.

3.2. Constrained optimization implementation

The LS problem with the proposed normalization constraint can be formulated as follows. The algebraic distances corresponding to the N frames of a single marker trajectory can be written using data matrix D as

$$\begin{bmatrix} \delta_1 \\ \vdots \\ \delta_k \\ \vdots \\ \delta_N \end{bmatrix} = \begin{bmatrix} w_1 & x_1 & y_1 & z_1 & 1 \\ \vdots & \vdots & \vdots & \vdots & \vdots \\ w_k & x_k & y_k & z_k & 1 \\ \vdots & \vdots & \vdots & \vdots & \vdots \\ w_N & x_N & y_N & z_N & 1 \end{bmatrix} \mathbf{u} = D\mathbf{u}, \quad (12)$$

where the k th row represents the k th time frame in the trajectory. We minimize the sum of squared algebraic distances to estimate the spherical fit \mathbf{u} , resulting in the objective cost function

$$f_3 = (D\mathbf{u})^T(D\mathbf{u}) = \mathbf{u}^T D^T D \mathbf{u} = \mathbf{u}^T S \mathbf{u}, \quad (13)$$

where S is the matrix $D^T D$. In addition, the normalization constraint in Eq. (9) can be expressed in quadratic matrix form using the constraint matrix C :

$$\mathbf{u}^T C \mathbf{u} = [a \ b \ c \ d \ e] \begin{bmatrix} 0 & & & -2 \\ & 1 & & \\ & & 1 & \\ & & & 1 \\ -2 & & & 0 \end{bmatrix} \begin{bmatrix} a \\ b \\ c \\ d \\ e \end{bmatrix} = 1. \quad (14)$$

The constrained optimization problem is then

$$\begin{aligned} &\text{minimize } \mathbf{u}^T S \mathbf{u} \\ &\text{subject to } \mathbf{u}^T C \mathbf{u} = 1. \end{aligned} \quad (15)$$

An equivalent unconstrained optimization problem minimizes the Lagrangian function

$$L = \mathbf{u}^T S \mathbf{u} - \lambda \mathbf{u}^T C \mathbf{u}, \quad (16)$$

where λ is the Lagrangian multiplier (see, e.g. Hillier and Lieberman, 2004). Differentiating with respect to \mathbf{u} yields the generalized eigenvalue problem

$$S\mathbf{u} = \lambda C\mathbf{u} \quad (17)$$

which can be solved with the QZ algorithm developed by Moler and Stewart (1973). The best-fit solution is the generalized eigenvector \mathbf{u} with non-negative eigenvalue λ which has the least cost according to Eq. (13) and subject to Eq. (14) (Bookstein, 1979; Fitzgibbon et al., 1999).

The CoR \mathbf{m} is calculated from the components of the selected coefficient vector \mathbf{u} by comparing Eqs. (6) and (7):

$$\mathbf{m} = (x_c, y_c, z_c)^T = -\frac{1}{2a}(b, c, d)^T. \quad (18)$$

Similarly, the radius can be calculated as

$$r^2 = \frac{e}{a} - \|\mathbf{m}\|^2. \quad (19)$$

4. Method for multiple markers

We extend the single sphere fit by Pratt (1987) to simultaneously fit spheres to multiple marker trajectories. For P concentric spheres with different radii, the first four basis function coefficients (a, b, c, d) parameterize the CoR, which is the sphere center common to all trajectories (Eq. (18)). Only the coefficient of the fifth basis function e is dependent on the individual radius values and hence will vary with each marker (Eq. (19)). Thus, to estimate the CoR and the multiple marker radii concurrently, we will solve for an augmented $(4 + P)$ coefficient vector:

$$\mathbf{u} = (a, b, c, d, e_1, e_2, \dots, e_P)^T. \quad (20)$$

The data matrix D is modified to incorporate the data for all P markers. We construct it by building a submatrix corresponding to the data from each individual marker. Let the $N \times 4$ matrix D^p contain the values of the first four basis functions (w, x, y, z) for the p th marker, and let $\mathbf{1}$ denote an N column vector of ones to represent the fifth basis function which is the constant term:

$$D^p = \begin{bmatrix} w_1^p & x_1^p & y_1^p & z_1^p \\ \vdots & \vdots & \vdots & \vdots \\ w_k^p & x_k^p & y_k^p & z_k^p \\ \vdots & \vdots & \vdots & \vdots \\ w_N^p & x_N^p & y_N^p & z_N^p \end{bmatrix}, \quad \mathbf{1} = \begin{bmatrix} 1 \\ \vdots \\ 1 \\ \vdots \\ 1 \end{bmatrix}. \quad (21)$$

The PN algebraic distances are

$$D\mathbf{u} = \begin{bmatrix} D^1 & \mathbf{1} \\ \vdots & \ddots \\ D^P & \mathbf{1} \end{bmatrix} \mathbf{u}, \quad (22)$$

where D is a $(PN) \times (4 + P)$ matrix.

We construct a constraint for multiple markers by using the summation of the analogous single marker constraints (Eq. (9)) to normalize the augmented coefficient vector \mathbf{u} :

$$\sum_{p=1}^P (b^2 + c^2 + d^2 - 4ae_p) = a^2 \sum_{p=1}^P (r_p)^2 = 1. \quad (23)$$

The constraint in Eq. (23) preserves the invariance to geometric similarities since the sum of squared radii does not change with translation or rotation of the data set. This makes it preferable to alternative constraint choices (e.g. see Pratt, 1987) which would result in

different estimates for different specifications of the reference frame. Furthermore, the associated singularity where all marker radii are zero is not expected to occur in experimental conditions.

The corresponding augmented square constraint matrix C is size $4 + P$:

$$C = \begin{bmatrix} 0 & & & -2 & \cdots & -2 \\ & P & & & & \\ & & P & & & \\ -2 & & & P & & \\ \vdots & & & & \ddots & \\ -2 & & & & & 0 \end{bmatrix}. \quad (24)$$

With the definitions of matrices D and C extended for the augmented coefficient vector \mathbf{u} , the same system developed for a single marker (Eqs. (15)–(17)) can be used to fit multiple marker trajectories simultaneously. The CoR is calculated as before from Eq. (18). The individual radius of each trajectory is calculated by

$$(r_p)^2 = \frac{e_p}{a} - \|\mathbf{m}\|^2. \quad (25)$$

5. Simulation and experimental validation

The constrained optimization method was compared to existing CoR estimation techniques using both synthetic data with controlled error and experimental motion capture data. For each simulated and experimental data set, we calculated the CoR from five functional methods: the MA method (Marin et al., 2003), the LS solution of Gamage and Lasenby (2002), IS optimization of the cost function in Eq. (2), the BC modification to LS (Halvorsen, 2003), and the normalization method (NM) for multiple markers proposed as the new method.

All five techniques were implemented with MATLAB 6.5 (Mathworks, Inc.; Natick, MA). The iterative searches for MA and IS were initialized with the LS solution by Gamage and Lasenby (2002) to be consistent with the BC algorithm which by construction begins with the Gamage and Lasenby (2002) solution. The procedures for MA and IS employ the MATLAB function *fminsearch*, which uses simplex direct search. The convergence criterion for BC was set to the same values as *fminsearch*. We compare the CoR locations estimated by each method as well as the required computation time on a 3 GHz Pentium 4 machine.

5.1. Simulated data

The method was first evaluated by its performance on synthetic data with controlled amounts of error. The

stationary CoR location was estimated by three marker trajectories for different RoMs and error amplitudes. We tested two sets of marker positions, motivated by a spherical joint model of the thumb carpometacarpal (CMC) joint (Fig. 2). The M marker set models markers on the thumb metacarpal segment (M1, M2, and M3) and the H marker set represents markers on the hand dorsum (H1, H2, and H3) (Table 1).

The generated marker trajectories simulated thumb circumduction by beginning from a nominal mean position and circling out to increasing angles relative to the mean position. The maximum angular RoMs tested were 5° , 15° , and 45° from the mean position (Fig. 3). There were 30 data sets (trials) generated with independent error sequences for each set of test conditions. All marker trajectories had 120 frames.

The simulation tests investigated the effect of isotropic pseudo-random errors in the marker position coordinates. We used a spherical model to generate error vectors which were added to the marker positions. The directions of the error vectors were uniformly distributed, and the magnitudes of the random errors were normally distributed with standard deviations of 0.5, 1.0, and 2.0 mm.

We use the distance between the estimated CoR and the nominal CoR, referred to as CoR error, to compare the accuracy of the five methods. The CoR is estimated by each method for the same 30 trials for a given error and RoM condition, and the average CoR error is calculated.

5.1.1. Simulation results

The CoR error generally increased with increasing error amplitude and decreasing RoM for all methods (Fig. 4). The BC method also required increasing numbers of iterations, and in particular it did not converge for several trials for the cases of 5° RoM with

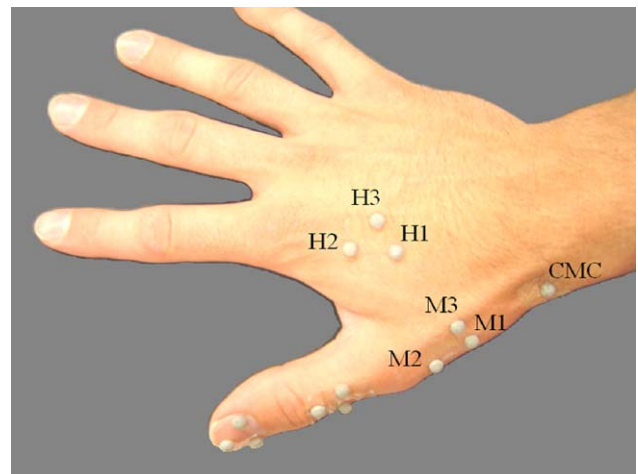


Fig. 2. Marker protocol modeled by synthetic data and used for empirical data.

Table 1
Simulated marker protocol parameters for a model of the thumb CMC joint

Marker set	Marker number		
	1	2	3
Distance from CoR (mm)			
Thumb metacarpal (M)	13.8	29.0	15.7
Hand dorsum (H)	48.7	56.7	69.1

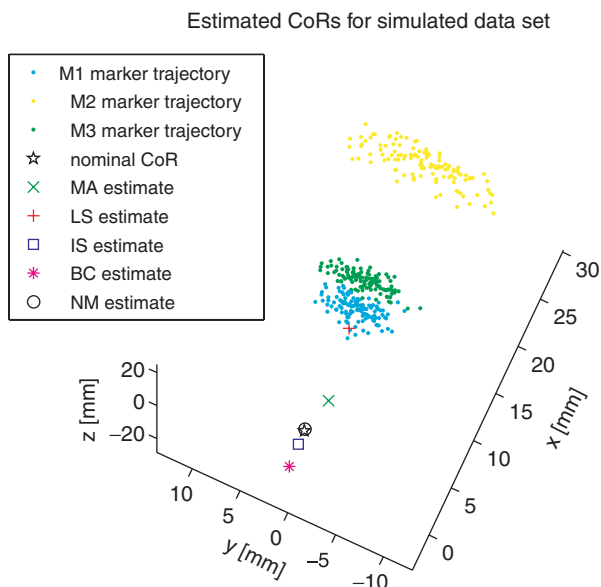


Fig. 3. Sample synthetic data set for $\pm 5^\circ$ RoM with 1.0 mm standard deviation of random error for the M marker set. LS estimates a CoR which is 10.9 mm away from the true nominal CoR. The proposed NM method's estimate has 0.3 mm CoR error, while the CoRs from the MA, IS, and BC iterative functional methods have 3.7, 1.4, and 3.7 mm CoR error, respectively.

1.0 and 2.0 mm standard deviation error in the M marker set tests. For these two most extreme error cases, all five methods performed poorly and had average CoR errors greater than 25 and 60 mm for the 1.0 and 2.0 mm error conditions, respectively. The mean CoR error was calculated from only the trials for which the BC solution did converge (Fig. 4).

CoR error for LS was progressively worse relative to the other non-rigid sphere-fitting methods, except for the test condition using the M marker set with the smallest RoM. MA compared well to the four sphere-fitting solutions for the M marker set, but exhibited CoR error up to 40 mm greater than the other methods for the H marker set. The mean CoR error for IS was the lowest of all five errors for more than 55% of the test cases. However, in the M marker set test, IS returned local minima for 42 of the converged trials and 17 trials within the 5° and 15° RoM conditions, respectively.

For the conditions for which all trials converged (Fig. 4), the absolute difference between the mean NM CoR

error and the best method's CoR error was less than 0.5 mm for 83% of the test conditions and at most 2.7 mm for all conditions. The mean computational time required to estimate the CoR was calculated for each method based on the performance for all of the converged data trials (Table 2). Our results suggest that the new method delivers performance similar to the best alternative in each test situation, without requiring additional computational time.

5.2. Empirical data

The method was also evaluated empirically using measured hand movement. Surface markers were placed on the hand of a normal subject around the thumb CMC joint as modeled in the simulation (Fig. 2). The true CoR location was not available, but an additional seventh marker at the base of the thumb approximated the CMC joint position. Marker trajectories were recorded for thumb movement in two sessions. In the first session with 775 frames, the subject was asked to exercise the full active RoM of the CMC joint. In the second session of 1255 frames, the subject used an external object against the thumb tip to exercise the full passive RoM. The previous section suggests that using the H marker set resulted in less error for the best method, so the trajectories of the hand dorsum markers in the frame of the thumb metacarpal segment were used for CoR estimation (Fig. 5).

The estimates were compared based on the distance from the mean position of the CMC marker trajectory (Table 3). LS estimates had a separation of almost 3 and 4 cm from the CMC marker, while the estimates of MA, IS, BC, and NM methods were at more plausible CMC CoR locations of about 1–2 cm away from the surface marker. The relative orders of magnitude for computational time were the same as that reported for the synthetic data simulations.

6. Discussion and conclusion

The cost function used in a CoR estimation method determines important mathematical properties of the solution, such as the accuracy, repeatability, and computational expense. The geometric error in Eq. (2)

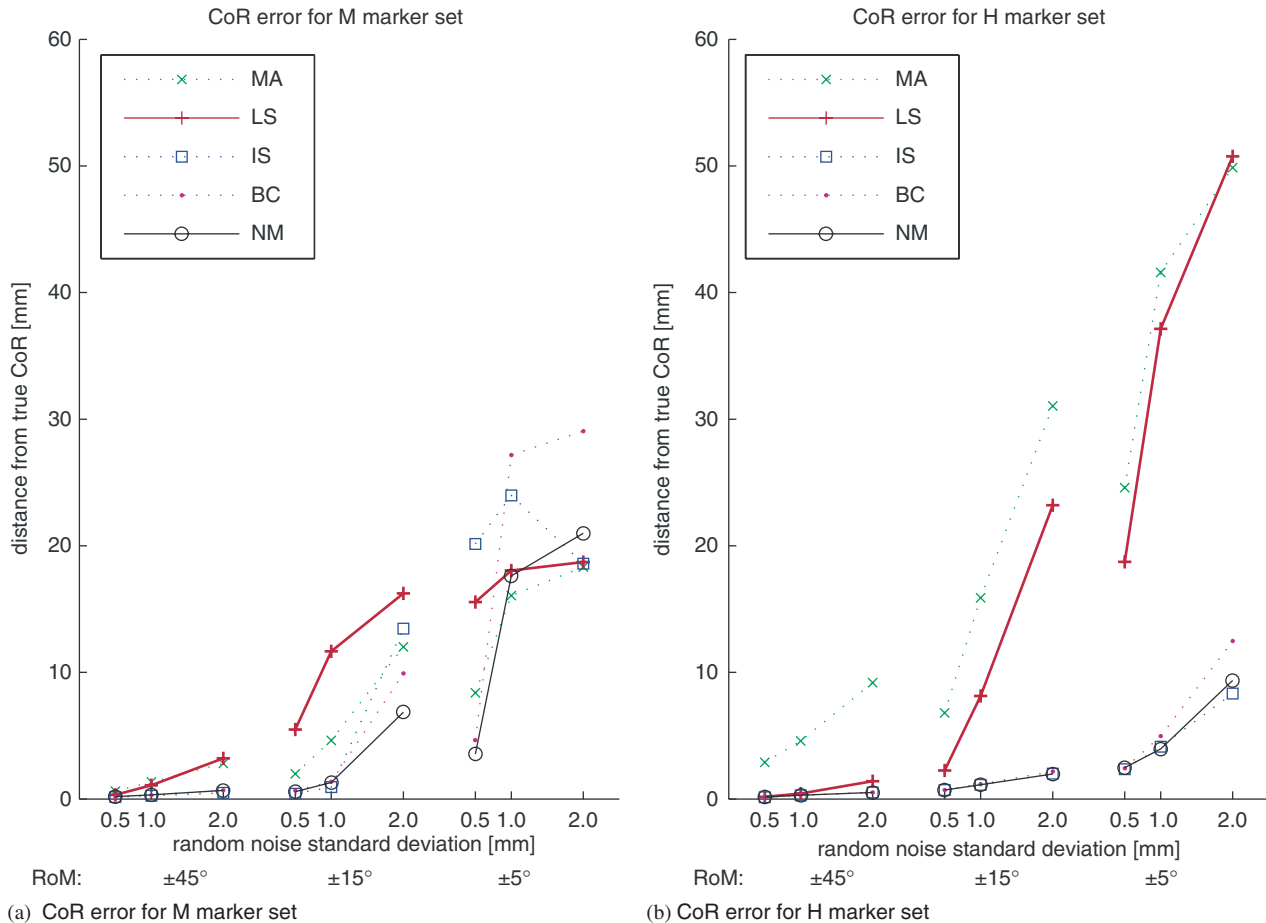


Fig. 4. Average distance of CoR estimate from true CoR for synthetic data with random normal error for (a) the M marker set and (b) the H marker set. For the M marker simulation with $\pm 5^\circ$ RoM, the CoR error is calculated for all methods from only the trials for which the BC solution converged: 30 trials, 16 trials, and 9 trials for the 0.5, 1.0, and 2.0 mm standard deviation error conditions, respectively.

Table 2
Computational time for the set of trials where the BC method converged

	Method				
	MA	LS	IS	BC	NM
Mean computation time for a single trial (s)	1.2	0.0056	0.079	0.12	0.00076

is a natural choice for cost function, but its structure precludes an exact formulation. Iterative algorithms can be used to optimize any cost function but may return a local minimum as the solution, as seen in our synthetic data experiments (Section 5.1.1). Though global search would avoid the problem of local minima, the additional computational expense may be unacceptable.

Exact formulations are preferable because the solutions are unique and thus repeatable, and the computation procedure is usually fast. The previously proposed LS method by [Gamage and Lasenby \(2002\)](#) exhibits all of these advantages, but the cost function has associated

flat plane singularities which result in inaccurate fits for data which have small RoM. Our experiments verify that this inaccuracy can be problematic for scenarios such as capturing the CoR of the thumb CMC joint, as plausible error conditions of $\pm 15^\circ$ RoM and 1.0 mm standard deviation of error resulted in 8 mm error (Fig. 4b). [Halvorsen \(2003\)](#) derives the BC algorithm to iteratively correct the LS solution, but the method is also sensitive to the choice of convergence parameters. For example, in some simulations of the most extreme error conditions, the BC method failed to converge (Section 5.1.1).

Estimated CoRs for CMC thumb joint from empirical surface marker data

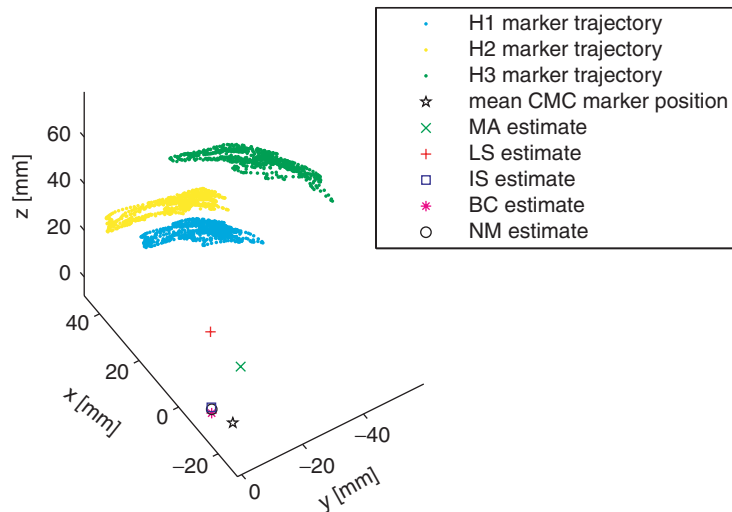


Fig. 5. The experimental data set where subject was asked to exercise full active RoM. The trajectories of the hand dorsum H marker set are plotted in the frame defined by the markers on the thumb metacarpal segment. The mean CMC marker position denotes the general location of the surface marker near the CMC joint (Fig. 2). The LS and MA estimates are farther from the CMC surface marker while IS, BC, and NM give similar estimates which are more plausible locations for the CoR relative to the CMC joint anatomy (Table 3).

Table 3
Empirical data results of CoR estimation for the thumb CMC joint

Data set	Method				
	MA	LS	IS	BC	NM
<i>Distance from CMC marker (mm)</i>					
Active	18.0	27.7	13.9	12.1	12.4
Passive	11.4	37.2	12.5	8.9	7.8

Our constrained least-squares optimization method is not subject to local minima. In addition, the solution does not rely on manually-adjusted optimization parameters. We use an objective cost function similar to that in [Gamage and Lasenby \(2002\)](#), but the mathematical formulation requires an explicit normalization scheme. The carefully chosen normalization constraint is invariant to geometric similarities and successfully avoids flat plane singularities associated with low RoM, without introducing singularities that are relevant to practical situations. In simulation tests of five methods, the new method yielded solutions with accuracy comparable to that of the best iterative alternatives and required the least computational time.

The comparative evaluation included the MA approach because of its alternative cost function which is not based on sphere fitting. In some cases the MA estimate had large errors of similar magnitude to the LS error. The discrepancy with the previous [Marin et al. \(2003\)](#) study may be due to the difference from their testing conditions, where markers were rigidly fixed to a

mechanical linkage. Further exploration is needed to test this hypothesis.

Work by [Camomilla et al. \(2006\)](#) suggests that accuracy of functional CoR estimation methods improves when the marker clusters have a wider spread and shorter distance from the CoR. These were competing factors between the two marker protocols tested in this study since the H markers had larger spread but were also further from the CoR than the M markers. Our results suggest that larger separation from the CoR was the dominant factor for LS and MA, which had decreased accuracy for the H marker set, while the wider marker spread was more critical for IS, BC, and NM, which had increased accuracy for the H marker set.

In summary, the accuracy of our approach for reduced RoM situations, along with the repeatability and speed of a least-squares solution, make the new method suitable for use in an automated skeletal extraction procedure for spherical and axial joints. In addition, the new method can provide an improved initial estimate for iterative searches which optimize cost functions with no exact solution.

Acknowledgements

This work was supported by the National Science Foundation (CCF-0343161, IIS-0326322, ECS-0325383, and CNS-0423546). L.Y. Chang is supported by the National Science Foundation Graduate Research Fellowship.

References

- Bell, A.L., Brand, R.A., Pedersen, D.R., 1989. Prediction of hip joint center location from external landmarks. *Human Movement Science* 8, 3–16.
- Bookstein, F.L., 1979. Fitting conic sections to scattered data. *Computer Graphics and Image Processing* 9, 56–71.
- Camomilla, V., Cereatti, A., Vannozzi, G., Cappozzo, A., 2006. An optimized protocol for hip joint centre determination using the functional method. *Journal of Biomechanics* 39, 1096–1106.
- Cerveri, P., Lopomo, N., Pedotti, A., Ferrigno, G., 2005. Derivation of centers and axes of rotation for wrist and fingers in a hand kinematic model: methods and reliability results. *Annals of Biomedical Engineering* 33, 402–412.
- Davis, R.B., Ounpuu, S., Tyburski, D., Gage, J., 1991. A gait analysis data collection and reduction technique. *Human Movement Science* 10, 575–587.
- Fitzgibbon, A.W., Pilu, M., Fisher, R.B., 1999. Direct least square fitting of ellipses. *IEEE Transactions on Pattern Analysis and Machine Intelligence* 21, 476–480.
- Gamage, S.S.H.U., Lasenby, J., 2002. New least squares solutions for estimating the average centre of rotation and the axis of rotation. *Journal of Biomechanics* 35, 87–93.
- Halvorsen, K., 2003. Bias compensated least squares estimate of the center of rotation. *Journal of Biomechanics* 36, 999–1008.
- Halvorsen, K., Lesser, M., Lundberg, A., 1999. A new method for estimating the axis of rotation and the center of rotation. *Journal of Biomechanics* 32, 1221–1227.
- Hillier, F.S., Lieberman, G.J., 2004. *Introduction to Operations Research*, eighth ed. McGraw-Hill, New York.
- Kadaba, M.P., Ramakrishnan, H.K., Wootten, M.E., 1990. Measurement of lower extremity kinematics during level walking. *Journal of Orthopedic Research* 8, 383–392.
- Marin, F., Mannel, H., Claes, L., Durselen, L., 2003. Accurate determination of a joint rotation center based on the minimal amplitude point method. *Computer Aided Surgery* 8, 30–42.
- Moler, C.B., Stewart, G.W., 1973. An algorithm for generalized matrix eigenvalue problems. *SIAM Journal on Numerical Analysis* 10, 241–256.
- Panjabi, M.M., 1979. Centers and angles of rotation of body joints: a study of errors and optimization. *Journal of Biomechanics* 12, 911–920.
- Piazza, S.J., Okita, N., Cavanagh, P.R., 2001. Accuracy of the functional method of hip joint center location: effects of limited motion and varied implementation. *Journal of Biomechanics* 34, 967–973.
- Pratt, V., 1987. Direct least-squares fitting of algebraic surfaces. *Computer Graphics* 21, 145–152.
- Reuleaux, F., 1876. *Kinematics of Machinery: Outlines of a Theory of Machines*. (A.B.W. Kennedy, Trans.). MacMillan and Co., London. (Original work published 1875).
- Silaghi, M., Planckers, R., Boulic, R., Fua, P., Thalmann, D., 1998. Local and global skeleton fitting techniques for optical motion capture. In: Magnenat-Thalmann, N., Thalmann, D. (Eds.), *Modelling and Motion Capture Techniques for Virtual Environments*, Lecture Notes in Artificial Intelligence, vol. 1537. Springer, Berlin, pp. 26–40.
- Vaughan, C.L., Davis, B.L., O'Connor, J., 1999. *Dynamics of Human Gait*, second ed. Kiboho Publishers, Cape Town, South Africa.
- Zhang, X., Lee, S.W., Braido, P., 2003. Determining finger segmental centers of rotation in flexion-extension based on surface marker measurement. *Journal of Biomechanics* 36, 1097–1102.